Journal of Membrane Science 594 (2020) 117438

Contents lists available at ScienceDirect

Journal of Membrane Science

journal homepage: www.elsevier.com/locate/memsci

A facile route to the preparation of antibacterial polysulfone-sulfonated polyethersulfone ultrafiltration membranes using a cationic surfactant cetyltrimethylammonium bromide

Aydın Cihanoğlu, Sacide Alsoy Altinkaya*

Department of Chemical Engineering, İzmir Institute of Technology, Gülbahçe Campus, 35430, Urla, İzmir, Turkey

ARTICLE INFO

Keywords:
Quaternary ammonium compounds
CTAB
Antibacterial membrane
Antibiofouling
Polysulfone
Sulfonated polyethersulfone
Membrane biofouling

ABSTRACT

Cetyltrimethylammonium bromide (CTAB), a cationic surfactant, is known to have strong bactericidal potential. In this study, we report a facile approach for preparing CTAB-containing polysulfone-sulfonated polyethersulfone (PSF-SPES) based ultrafiltration membranes with antibacterial properties. The CTAB was added in gelation medium at three different concentrations and made an electrostatic interaction with SPES at the polymer/bath interface during phase inversion. The successful incorporation of the CTAB in the membrane structure was confirmed by attenuated total reflectance Fourier transform infrared spectroscopy and X-ray photoelectron spectroscopy. The CTAB-containing membranes had higher contact angle, lower pure water permeability (PWP) and molecular weight cut-off than the pristine membrane. The membranes prepared at critical and above critical micelle concentration (CMC) of the CTAB showed excellent antibacterial activity on both Gram-negative (*Escherichia coli*) and Gram-positive (*Staphylococcus aureus*) bacteria. On the other hand, the PWP of the membrane decreased from 93 ± 1.6 to 39.3 ± 3.2 $L/m^2 h$ bar upon increasing the CTAB concentration from 10^{-3} M (=CMC) to 10^{-2} M, consequently, CMC was chosen as the optimal concentration. The membrane prepared at the CMC displayed almost 100% flux recoveries after dynamic bacteria filtration followed by simple rinsing with PBS solution. Leaching experiments continued up to 30 days demonstrated that 96% of the CTAB remained in this membrane. Furthermore, at the end of 1 month of storage in 1 M NaCl solution, no change was observed in the antibacterial activity of this membrane compared to fresh membrane. These findings emphasize the potential of the facile approach proposed in this study to develop antibacterial ultrafiltration membranes in a single step.

1. Introduction

Biofouling due to attachment of living microorganisms and subsequent cohesive biofilm formation on membrane surfaces is a serious problem limiting the cost effectiveness of membrane technology. Various approaches have been developed to suppress biofouling including pre-treatment of feed solution, optimization of operating conditions, periodically cleaning membrane and using antibiofouling membranes [1–5]. Among these strategies, fabricating antibiofouling membranes is an attractive alternative since other solutions require high cost, delicate operation and use of toxic chemicals. Antibiofouling membranes are developed by introducing antibacterial agents on the surface or in the bulk structure of membranes [6]. These types of membranes kill bacteria through release of active agents (release-killing) or direct contact of active agents with bacteria (contact-killing). In release-killing approach, continuous release of antibacterial agent results in a shorter lasting period of the membrane and causes an environmental risk. Therefore, recent studies focused on developing membranes with stable and long-lasting antibacterial activities through contact-killing properties.

Various bactericidal components such as graphene oxide [7], carbon nanotube [8,9] antimicrobial polymers [10] and quaternary ammonium compounds (QACs) [11] have been used to develop antibacterial membranes capable of inactivating microorganisms upon contact. Among these agents, QACs are promising candidates due to their high antibacterial efficiency, lack of skin irritation, non-toxic behavior and low cost. In literature different QACs have been integrated into membranes through in-situ membrane modification during preparation [12,13], coating [14,15] and grafting [16–18] on the membrane surface or quaternized polymers have been used for membrane preparation

* Corresponding author.
E-mail address: sacidealsoy@iyte.edu.tr (S.A. Altinkaya).

https://doi.org/10.1016/j.memsci.2019.117438
Received 1 May 2019; Received in revised form 3 August 2019; Accepted 31 August 2019
Available online 06 September 2019
0376-7388/

[19,20]. Quaternization of poly(vinyl chloride) ultrafiltration membranes through post treatment by soaking commercial PVC hollow fiber membranes in trimethylamine solution changed the bulk structure of the membrane by blocking the pores [14]. Covalent immobilization of 3-chloro-2-hydroxypropyl-trimethyl ammonium chloride (CHPTAC) onto partially hydrolysed cellulose triacetate reverse osmosis membranes had an etching effect on the surface of the membrane resulting in a decrease in the thickness of dense top layer [16]. Other than causing changes in the bulk and surface structure, coating and grafting techniques require abundant chemical usage and utilize a lengthy procedure for preparing the membranes. The QAC was blended into the casting solution without any modification [19] or after being immobilized on a support [13,19,20]. The major drawback of the physical blending technique is considered to be distribution of contact-killing antibacterial compound through the membrane cross section, hence, its insufficient concentration on the surface. To overcome this disadvantage, Zhang et al. proposed triggering surface segregation of the QAC. For this purpose, they first produced a carbon support by ultrasonic spray pyrolysis, modified the support by oxidizing in $KMnO_4$ and $NaNO_3$ in concentrated H_2SO_4 and then immobilized the QAC on this support. Finally, the membrane was prepared by mixing this QAC@-Carbon composite into polyvinylidene fluoride (PVDF) [13]. Although physical blending is a simple technique, the substantial pre-treatment steps for the preparation of the QAC or the polymer including QACs hamper simplicity of the method. The current state of the art indicates that to commercialize antibacterial membranes with contact-killing properties there is still a need for new manufacturing protocols which can easily be scaled up without any change in production lines and significant increase in the production time. Pre-treatment or post treatment of the antibacterial agent and/or membrane increases manufacturing cost, as a result reduces the possibility of scale up and commercialization.

In this study we report a facile approach for developing stable antibiofouling membranes in a single step. Prior studies added QACs into casting solution, instead, we dissolved cetyltrimethyl ammonium bromide (CTAB) in the coagulation bath. We hypothesize that when the casting solution prepared from polysulfone (PSF) and sulfonated polyethersulfone (SPES) is immersed into the coagulation bath, hydrophilic polymer SPES diffuses towards coagulation bath/polymer solution interface faster than hydrophobic PSF. This allows electrostatic interaction between positively charged quaternary ammonium group (NR_4^+) in CTAB and negatively charged sulfonic acid (SO_3^-) group in SPES to occur mostly at the interface which in turn lead to accumulation of CTAB on the surface. With our approach the CTAB-containing antibacterial membrane is prepared in a single step through classical phase inversion process and the leakage of CTAB is prevented through its electrostatic attachment to the SPES. Compared to prior studies, our strategy does not require pre-treatment or grafting of QAC on a support to maintain stability and high antibacterial activity at the surface. We added CTAB in the coagulation bath at its critical micelle concentration (CMC) and significantly below (LCMC) and above the CMC (HCMC). The resulting membranes were characterized in terms of their fluxes, molecular weight cut-off values, morphology and surface properties. Based on flux data and static antibacterial activities against Gram-positive (*Staphylococcus aureus*) and Gram-negative (*Escherichia coli*) bacteria, optimum CTAB concentration was determined. The membrane prepared at the optimum concentration was further characterized to evaluate its antibiofouling performance and stability. To the best of our knowledge, the facile approach proposed in this study has been applied for the first time to incorporate QAC into polymer membranes. This approach offers a simple route to prepare antibiofouling membranes and can be easily scaled up for industrial production.

2. Materials and methods

2.1. Materials

PSF (Mw = 35 kDa) purchased from Sigma-Aldrich and SPES (Mw = 80 kDa, Sulfonation degree (SD) < 30%) kindly donated by Konishi Chemicals, Japan were used to prepare flat sheet ultrafiltration membrane. 1-methyl-2- pyrrolidone (NMP, 99.5%) and N, N-Dimethylacetamide (DMAc, 99%) purchased from Fluka and Sigma-Aldrich, respectively were used to dissolve PSF and SPES. CTAB was used as an antibacterial agent and supplied by Alfa Aesar. Polyethylene glycols (PEGs) with different molecular weights (1 kDa (Sigma-Aldrich), 4 kDa (Merck), 6 kDa (Merck), 10 kDa (Sigma-Aldrich), 20 kDa (Sigma-Aldrich), and 35 kDa (Sigma-Aldrich)) and Polyethylene oxide (PEO) (100 kDa (Sigma-Aldrich)) were used for determining molecular weight cut-off of the prepared membranes. NaCl and Phosphate Buffered Saline (PBS) were obtained from Sigma-Aldrich and used for testing the stability of the CTAB and for rinsing the membrane after bacteria filtration, respectively. Gram-negative (*Escherichia coli*, ATCC 25922) and Gram-positive (*Staphylococcus aureus*, RSKK 1009) bacteria used as model microorganisms for antibacterial tests were received from Biotechnology Research Center (BIOMER) of İzmir Institute of Technology.

2.2. Preparation of CTAB-containing ultrafiltration membranes

Membranes were prepared from a blend of PSF and SPES by non-solvent phase inversion technique. The PSF:SPES blending ratio was adjusted to 3:1. Polymers were first dried in a vacuum oven at 80 °C for 24 h to remove moisture and dissolved (25 wt%) in DMAc and NMP (DMAc:NMP ratio of 2:1) by stirring at 100 rpm for 24 h. In order to eliminate air bubbles in the casting solution, the solution was held for 24 h without stirring. Next, the solution was cast on a clean glass plate using automated film applicator (Sheen Instrument Ltd., model number: 1133 N) and the casting thickness was adjusted to 250 μm by a four-sided applicator. Following casting, the glass plate was immediately immersed into the coagulation bath containing CTAB dissolved in water and kept in the bath for 24 h. The CTAB concentration was adjusted to 10^{-4} M, 10^{-3} M and 10^{-2} M and the resulting membranes were coded as MQ_{LCMC}, MQ_{CMC}, MQ_{HCMC}, respectively. The pristine membrane coagulated in the absence of the CTAB just in deionised (DI) water was denoted as M0. The obtained membranes were rinsed several times with DI water to remove loosely bound CTAB molecules, and stored in DI water at 4 °C (refrigerator) until further tests. A facile route to the preparation of antibacterial PSF-SPES ultrafiltration membranes using CTAB is shown in Scheme 1.

2.3. Membrane filtration performance

The filtration performance of the pristine and modified membranes was carried out using a dead-end cell filtration system (Millipore, Amicon Stirred Cell 8010). Each membrane was compacted to reach steady state conditions prior to any filtration test. Then, pure water was filtered at 1 bar and collected permeate volume was recorded for specific time intervals. The volumetric flux was calculated from the slope of the permeate volume vs. time graph and converted to hydraulic pure water permeability (PWP) using following equation:

$$PWP = \frac{\Delta V}{A \Delta t \Delta P} \quad (1)$$

where ΔV is the volume of permeated water (L), A (m^2) is the membrane area, Δt (h) is the permeation time and ΔP (bar) is the transmembrane pressure difference applied through the membrane ($n = 3$ where n is the number of repeated experiments). To determine molecular weight cut-off (MWCO) of the membranes, 10 mL of 1 g/L aqueous solutions of neutral PEG molecules with different molecular

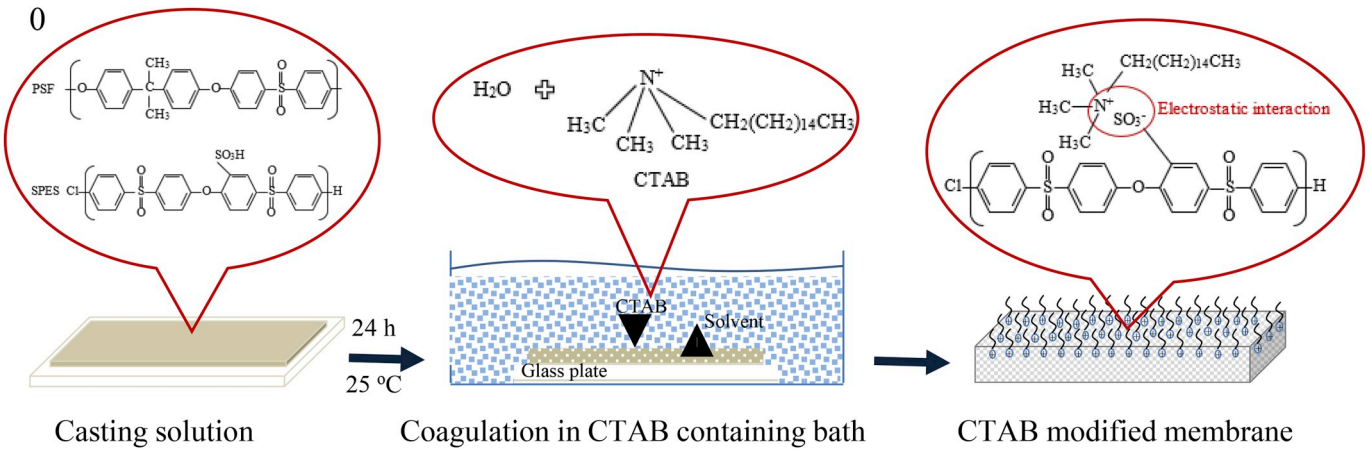

Scheme 1. The protocol used for preparing CTAB containing membranes.

weights were filtered at 1 bar until 5 mL of permeate was collected ($n = 3$). To ensure that the membrane was fully conditioned with PEG 1000, fresh solution was filtered three times. The concentrations of permeate, retentate and feed solutions were measured by Rudolph-J357 Automatic Refractometer. The solute rejection (%) was calculated using the equation:

$$R(\%) = \left(1 - \frac{C_p}{\frac{C_f + C_r}{2}}\right) x100 \quad (2)$$

where C_p, C_r and C_f are the concentrations of permeate, retentate and feed solution, respectively. To eliminate concentration polarization, the solution was stirred at 300 rpm.

The pore radius distribution of the membranes was calculated using the probability density function based on the assumption of no interaction (steric and hydrodynamic) between the neutral PEG molecules and pores of the membranes [21].

$$\frac{dR(r_p)}{dr_p} = \frac{1}{r_p x ln\sigma_p x\sqrt{2\pi}} exp\left[-\frac{(lnr_p - ln\mu_p)^2}{2x(ln\sigma_p)^2}\right] \quad (3)$$

where μ_p is the mean effective pore radius determined at the PEG rejection coefficient of 50% and σ_p is the geometric standard deviation defined as the ratio of radius r_p at the PEG rejection of 83.14% over that at 50%.

The stokes radius of the neutral PEG molecules can be calculated through the following equation:

$$r_p = 16.73x10^{-12} x MW^{0.557}, (MW \leq 35000) \quad (4)$$

The porosity of the membranes (ε) was calculated from weight and thickness measurements as follows [22]:

$$\varepsilon = \frac{W_w - W_d}{S \times d \times \rho_w} \quad (5)$$

where W_w and W_d are the weights of the wet and dry membranes, respectively, S is the area of the membranes, d is the average thickness of the membranes and ρ_w is the density of water (0.998 g/cm^3).

2.4. Membrane characterization

The chemical structure of the pristine and modified membranes was determined by Attenuated Total Reflectance Fourier Transformed Infrared Spectrometer (ATR-FTIR), (PerkinElmer). The spectrums of the membranes were collected at ambient temperature over a scanning range of 4000–650 cm^{-1} with a resolution of 4.0 cm^{-1}. Prior to analysis, all the membranes were dried in a vacuum oven (Memmert) at 25 °C. The surface charge of the membranes was determined by streaming potential measurements (NanoPlus Micromeritics Instrument) using 10^{-2} M NaCl (pH 7.4) as an electrolyte solution ($n = 3$). Water contact angle of the membranes was measured (Attension Optical tensiometer) with 5 μL water droplet after drying the membranes in a vacuum oven at 25 °C ($n = 5$). The surface and cross-section morphology of the membranes were characterized using a scanning electron microscope (SEM) (FEI Quanta 250 FEG). Before imaging, dried membranes were coated with gold using a Magnetron Sputter Coating Instrument. The surface roughness (R_a = arithmetic mean roughness, R_q = root-mean-square roughness) of the membranes was determined for a 5 × 5 μm^2 surface using atomic force microscopy (AFM) (MMSPM Nanoscope 8, Bruker) ($n = 3$). The elemental composition of the membrane prepared at the CMC (MQ_{CMC}) was determined using X-ray photoelectron spectra (XPS) (Thermo Scientific) at the emission angles of 0°, 15°, 30° and 45°. The amount of CTAB loaded into the membrane was determined using TGA analysis (Setaram, Labsys, TG-DTA/DSC). The heating rate was adjusted to 10 °C/min between 25 °C to 800 °C.

2.5. Antibacterial activity assessment of membranes

The antibacterial activities of the membranes were determined with colony-counting method according to ASTM E2180 standard protocol. Briefly, *E. coli* (Gram negative) and *S. aureus* (Gram positive) were inoculated in Mueller-Hinton agar at 37 °C. After incubation, bacteria colonies were picked off with a swab and mixed with 0.1% (w) peptone water to adjust concentration to the value of 0.5 in the McFarland standards scale. Then, bacteria suspensions were serially diluted with Mueller-Hinton broth to obtain final concentrations of 3.5 × 10^6 and 4.2 × 10^6 CFU/mL for *E. coli* and *S. aureus,* respectively.

Membrane coupons (effective area 3 cm × 3 cm) were first sterilized with UV light for 30 min and placed on agar plates. Next, the active side of the coupons were contacted with 300 μL of bacteria suspension for 24 h at 37 °C. Following incubation, the membranes were transferred into Erlenmeyer flasks containing 50 mL phosphate buffered saline solution (PBS, pH = 7.4) and sonication was applied for 10 min to remove deposited bacteria from the membrane surface. Finally, the bacteria suspension was spread on a LB plate, incubated for 24 h at 37 °C and the colonies were counted. The bactericidal rate was calculated using the following equation:

$$Antibacterial\ rate\ (\%) = \left(\frac{N_P - N_M}{N_P}\right) x100 \quad (6)$$

where N_P and N_M are the number of visual bacterial colonies on the agar plate after contacting with the pristine and modified membranes, respectively ($n = 3$).

2.6. Stability of the CTAB-containing membranes

The long-term stability of the CTAB-containing membrane was determined by measuring the CTAB released from the membrane. After storing membrane coupons in DI water for 1, 3, 7 and 30 days, the leached CTAB in water was measured with Total Organic Carbon (TOC) analyser. In addition, the membrane was stored in 1 M NaCl for 15 days at 4 °C and 30 days at 25 °C in a refrigerator and 1 M NaCl solution (1 L) was filtered through the membrane at 25 °C. At the end of static storage and dynamic salt filtration, the antibacterial activities of the used membrane against *E. coli* and *S. aureus* were measured. The amount of CTAB loaded into the membrane was calculated from the weight loss determined by TGA analysis.

2.7. Analysis of antibiofouling performance

The dynamic biofouling potentials of the M0 and MQ_{CMC} membranes were evaluated in a dead-end cell filtration system with a cell volume of 50 mL and an effective surface area of 13.4 cm^2 (Millipore, Amicon Stirred Cell 8050). Prior to experiments, membrane coupons were sterilized with UV light for 20 min. *E. coli* and *S. aureus* bacteria suspensions were prepared in PBS (pH 7.4) to reach concentrations of 1.75×10^8 and 2.1×10^8 CFU/mL, respectively. The biofouling experiment was carried out using 250 mL bacteria suspensions under similar initial fluxes for the pristine and the CTAB-containing membranes. Following filtration, the membrane coupons were rinsed with PBS for 10 min and water flux was re-measured to calculate the flux recovery ratio (FRR). Total fouling (R_{total}), reversible fouling (R_{rev}), irreversible fouling (R_{irrev}) and flux recovery ratios (FRR) were calculated using Eqs. (7)–(10).

$$R_{total}(\%) = \left(1 - \frac{J_P}{J_W}\right)x100 \tag{7}$$

$$R_{rev}(\%) = \left(\frac{J_R - J_P}{J_W}\right)x100 \tag{8}$$

$$R_{irrev}(\%) = \left(\frac{J_W - J_R}{J_W}\right)x100 \tag{9}$$

$$FRR(\%) = \left(\frac{J_R}{J_W}\right)x100 \tag{10}$$

where J_W is the pure water flux of the clean membrane, J_P is the flux of the bacteria suspensions passing through the membrane and J_R is the pure water flux of the washed membrane. The experiments were carried out at ambient temperature.

3. Results and discussion

3.1. Characterization of membranes

Fig. 1 shows the ATR-FTIR spectra for the pristine (M0) and CTAB-containing membranes. The peaks appeared at around 2925 cm^{-1} and 2853 cm^{-1}, assigned to the C–H symmetric and asymmetric stretching present in CH_2 group, confirmed the presence of CTAB in the membranes. The intensity of these peaks depends on the amount of CTAB added into the coagulation bath. As shown in Table 1, the higher CTAB concentration in the coagulation bath (< CMC, = CMC and > CMC) the larger the peak areas for both the C–H symmetric and asymmetric stretching. The increase in peak areas can be attributed to more electrostatic interaction formed between positively charged quaternary ammonium group in the CTAB (NR_4^+) and negatively charged sulfonic acid group in the PSF-SPES (SO_3^-) (Scheme 1).

The surface charge of the membranes determined at pH 7.4 is shown in Fig. 2. The pristine membrane (M0) has a negative charge (-22.21 ± 0.77 mV) due to deprotonation of the sulfonic acid group in SPES. Coagulation in the presence of CTAB allows obtaining membranes with an active layer formed via an electrostatic interaction between CTAB and SPES. Consequently, the surface charge of the CTAB-containing membranes shifted towards positive values.

The hydrophilicity of the membranes decreased in the presence of CTAB as demonstrated by the increased contact angle values (62.6 ± 3.9, 69.4 ± 1.1, 72.6 ± 1.3, 80.2 ± 1.5 for M0, MQ_{LCMC}, MQ_{CMC}, MQ_{HCMC} membranes, respectively) in Fig. 3. Hydrophilic quaternary ammonium head in the structure of the CTAB interacts with sulfonic acid group on the membrane surface and hydrophobic tail becomes free. This free tail makes the surface of the CTAB-containing membranes more hydrophobic than the pristine membrane.

The cross-section and surface morphologies of the membranes are shown in Figs. 4 and 5. For all membranes, a typical dense skin layer on the top surface and finger like structure in the sublayer were observed. A closer look at the structure nearby the surface with the higher magnification SEM images (x20000) showed the influence of the coagulation bath composition. With the increased CTAB concentration, the density of spongy pores increased, in addition, the small pores located in the finger-like cavities decreased. As shown in red frame in Fig. 4, almost all the pores in the finger like structure of the membrane prepared with the highest CTAB concentration (MQ_{HCMC}) disappeared compared to the pristine membrane (M0). The disappearance of finger-like pores in the sublayer of the CTAB-containing membranes is related with the decrease in the surface tension of the coagulation bath. It was reported that the surface tension of water is reduced from 72.8 dyne/cm to 37 dyne/cm by adding 10^{-2} M CTAB into water [23]. As discussed by Matz [24], the finger like pores and large macrovoid formation in the membrane structure occur due to hydrodynamic interfacial instabilities. In the presence of CTAB, such interfacial instabilities, as a result, tendency of finger like-cavity formation were reduced. Adding CTAB into the coagulation bath also changed the kinetics of phase inversion. The CTAB in gelation medium made electrostatic interaction with the SPES at the interface, hence, formed a barrier layer and slowed down the exchange of solvent/nonsolvent (Scheme 2). This delayed the precipitation and as shown in Table 2 caused the pore size of the skin layer to become smaller and porosity of the membrane to decrease. Surface SEM images in Fig. 5 demonstrate that the pristine (M0) membrane has the largest pore size. Compared to most of the Loeb-Sourirajan phase separation membranes often having an average porosity of 0.7–0.8 [25], the overall porosities of the pristine and CTAB containing membranes were found lower since no pore formers were used in the casting solution.

AFM images of the membranes are shown in Fig. 6. The roughness parameters listed in Table 2 for the CTAB modified membranes were found lower compared to that of the pristine membrane which confirms strong interaction between the CTAB and SPES at the surface.

3.2. Pure water permeability (PWP) and molecular weight cut-off (MWCO) of membranes

The pure water permeability of the pristine membrane was found to be 182.4 ± 8.3 L/m^2hbar. As shown in Fig. 7, the permeability decreased to 127.4 ± 3.2, 93.2 ± 1.6 and 39.3 ± 3.2 L/m^2hbar for the membranes coagulated in CTAB-containing bath at concentrations below (MQ_{LCMC}), at (MQ_{CMC}) and above (MQ_{HCMC}) the critical micelle concentration of the CTAB, respectively. The decline in permeability can be mainly explained by the increase in hydrophobicity of the membranes as confirmed with the increased contact angle values of the membranes (Fig. 3). In addition, the disappearance of small pores in the sublayer of the membranes can also account for the dramatic flux decline. Fig. 8 illustrates the rejection of six different PEGs (molecular weights 1, 4, 6, 10, 20, 35 kDa) and PEO (100 kDa) by the pristine and modified membranes. The MWCO of the membranes, defined as the molecular weight at which 90% of the solute is rejected by the membrane [26] were determined to be 30.5 kDa, 27.1 kDa, 27.4 kDa and

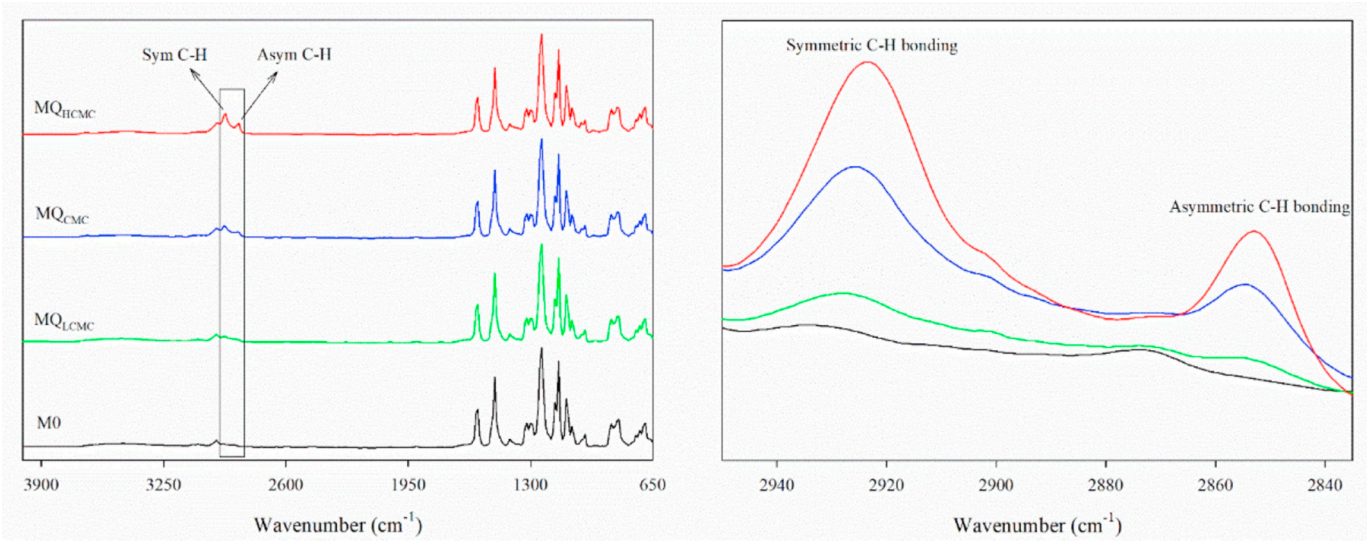

Fig. 1. ATR-FTIR spectra of the pristine and CTAB modified membranes.

Table 1
Peak areas for the pristine and CTAB-containing membranes.

Membranes	Peak Area	
	Sym C–H stretching ($2925\ cm^{-1}$)	Asym C–H stretching ($2853\ cm^{-1}$)
M0	–	–
MQ_{LCMC}	0.10	0.01
MQ_{CMC}	0.33	0.13
MQ_{HCMC}	0.64	0.23

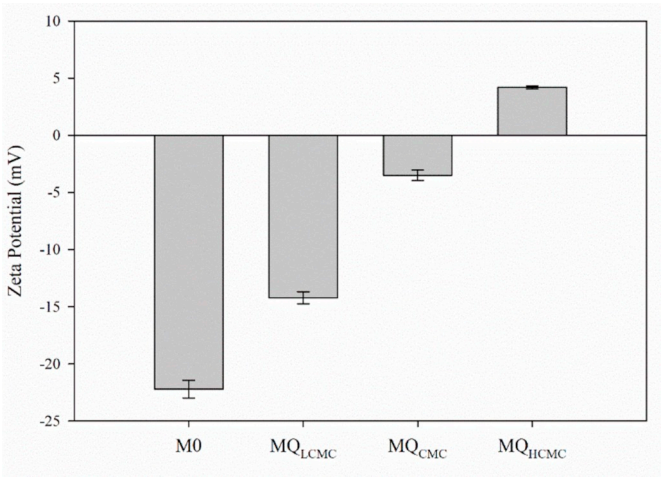

Fig. 2. Zeta potential of the pristine and CTAB modified membranes at pH 7.4.

21.4 kDa for the M0, MQ_{LCMC}, MQ_{CMC} and MQ_{HCMC}, respectively. As expected, smaller pore size and lower porosity of the CTAB containing membranes resulted in lower MWCO values as compared to that of the pristine membrane. In the presence of CTAB at the CMC (the CTAB is in spherical shape in the bulk phase) or below the CMC (the CTAB has a rod like shape in the bulk phase) in the coagulation medium, the barrier effect of CTAB on the exchange of solvent/nonsolvent is similar. Consequently, the MWCO values of the membranes prepared under these conditions (MQ_{LCMC}, MQ_{CMC}) were found the same. On the other hand, above the CMC, the shape of CTAB molecules changes from spherical to cylindrical [27], they form micelles in gelation medium and rate of exchange of solvent and nonsolvent, is significantly hindered due to

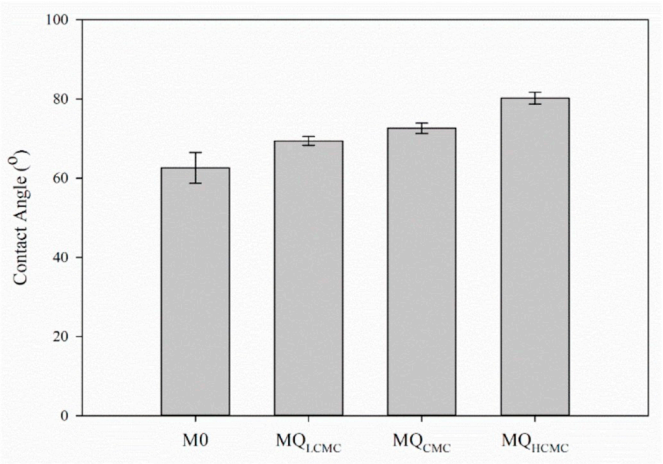

Fig. 3. Water contact angle of the pristine and CTAB modified membranes.

thicker adsorbed CTAB layer (Scheme 2c). As a result, the MQ_{HCMC} has a smaller MWCO value than the other CTAB-containing membranes. In the presence of highest CTAB concentration (10 x CMC) in gelation medium, the mean effective pore radius of the membranes decreased from 3.21 nm to 2.79 nm. On the other hand, the pore size distributions of the membranes were found similar regardless of the coagulation condition (Fig. 8).

3.3. Antibacterial activity assessment of the membranes

The antibacterial activities of the pristine and CTAB modified membranes were tested using Gram-negative (*E. coli*) and Gram-positive (*S. aureus*) bacteria. The pristine membrane did not inhibit the growth of bacteria. As shown in Table 3, the CTAB concentration below the CMC was insufficient to create a fully antibacterial surface (inhibition rate for *E coli* and *S. aureus* are 87.35% and 27.5%, respectively). On the other hand, the membranes prepared at (MQ_{CMC}) and above the CMC (MQ_{HCMC}) showed excellent growth inhibition both on *E. coli* and *S. aureus*. compared to the inhibition values reported in literature (Table 3).

The difference in the performance of the membranes listed in Table 3 can be explained by the method used for incorporating antibacterial agents. In previous studies, antibacterial agents were blended with polymers and distributed through the cross section [28–30], hence

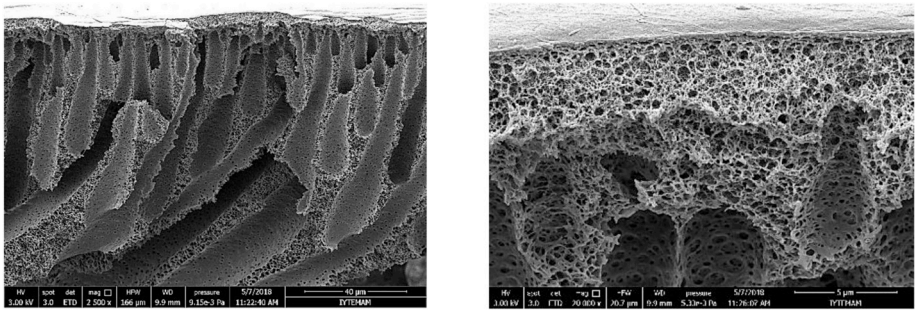

M0

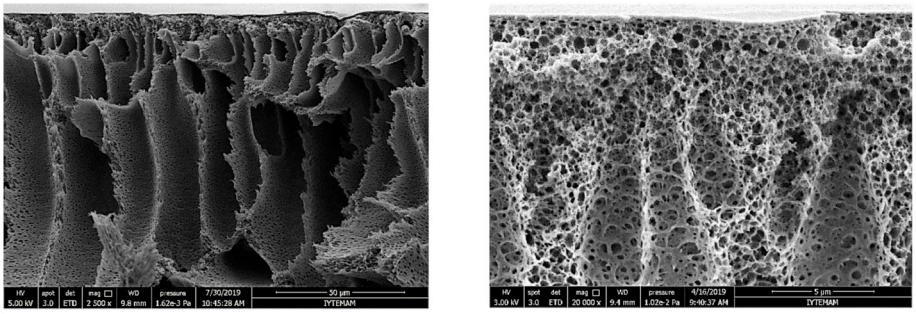

MQ_{LCMC}

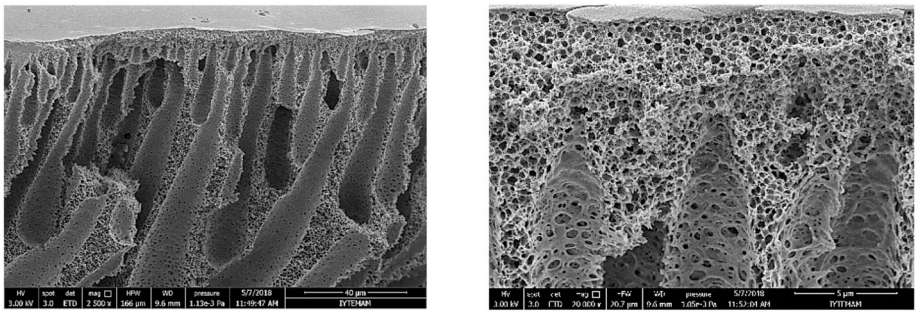

MQ_{CMC}

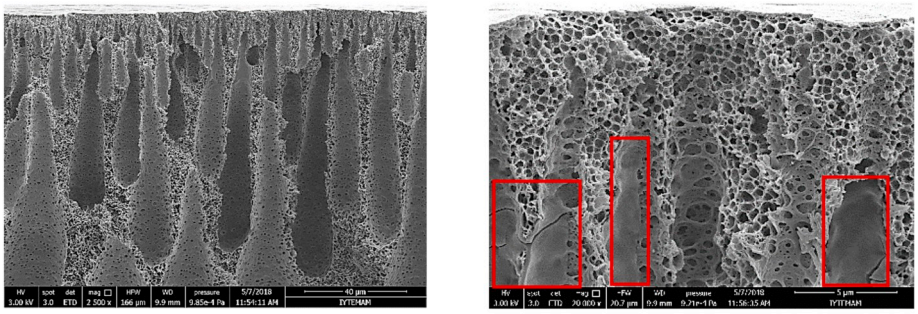

MQ_{HCMC}

Fig. 4. Cross-sectional SEM images of the pristine and CTAB modified membranes.

their surface concentration becomes insufficient. In our study, the active agent CTAB was added into the coagulation bath. During the coagulation step, the SPES selectively migrates to the interface due to its low surface energy. On the other hand, prior to phase inversion it is transported more slowly from the surface into the casting solution than the hydrophobic PSF [39]. This results in surface enrichment of the hydrophilic SPES, hence, the accumulation of the CTAB at the surface due to electrostatic interaction between the CTAB and SPES (Scheme 1). To prove our hypothesis, XPS analysis was carried out at four different angles (0°, 15°, 30° and 45°) (Fig. 9) to determine the near-surface composition of the membrane MQ_{CMC}. As illustrated in Table 4, % of nitrogen element which comes from the CTAB was found highest at 45°. The analysis of the data collected at 45° demonstrated that near-surface coverage of 68.7 wt% is achieved with a very low CTAB concentration of 0.036 wt% in the coagulation bath. The fraction of the CTAB at the surface is expected to be even higher, since the 45° take off angle used in the experiment takes into account contributions from a depth of 50 Å [39].

Based on XPS data Zhang et al. [13] reported QAC/PVDF ratio at the surface as 6.8% when QAC was blended into PVDF. They demonstrated that the rate of segregation of QAC to the surface can be increased by immobilizing it on a hydrophilic carbon material (QAC@Carbon). In

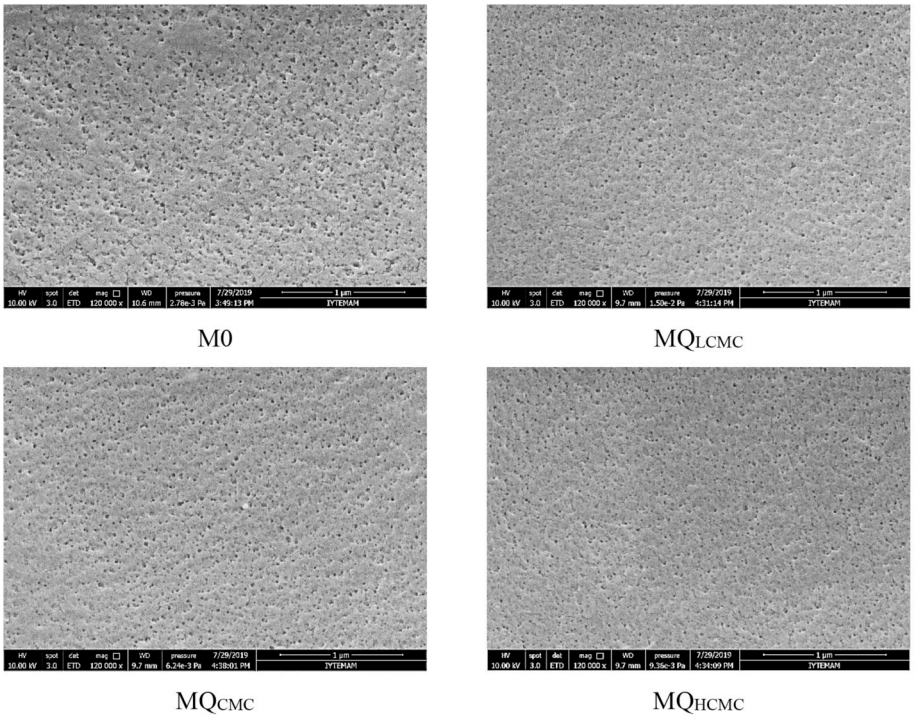

Fig. 5. Surface SEM images of the pristine and CTAB modified membranes.

this case QAC@Carbon/Polymer ratio was determined as 15.1% while in our case CTAB/Polymer ratio is 24.3%. These results clearly indicate the advantage of our approach in incorporating the QAC into the membranes. It should be noted that even though our membranes were prepared in a single step, they exhibited higher antibacterial performance than the thin film composite membranes [31,32] where the antibacterial agent is located on the surface in direct contact with the bacteria (Table 3). The superior performance can be attributed to both

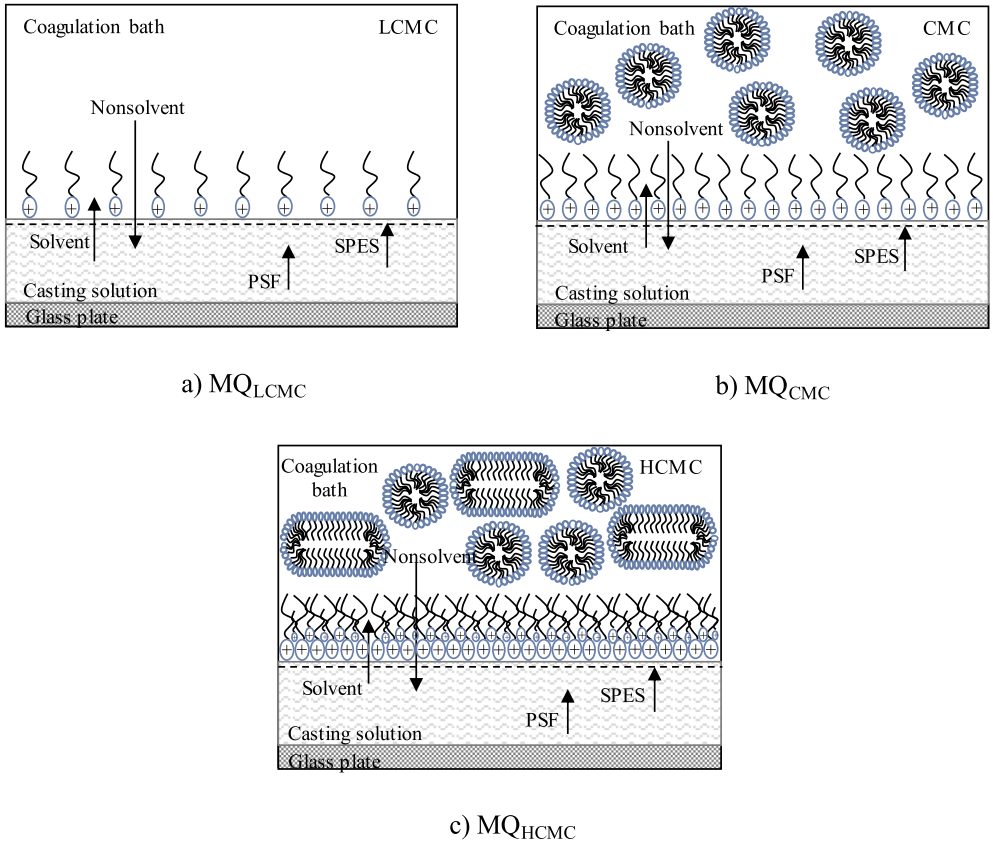

Scheme 2. The effect of CTAB concentration in coagulation bath on the rate of exchange of solvent/nonsolvent and accumulation of CTAB on the surface.

Table 2
Porosity, pore size and roughness of the pristine and CTAB modified membranes.

Membranes	Porosity, ε %	Pore radius (nm)	Ra (nm)	Rq (nm)
M0	43.1	3.21	4.99 ± 0.17	6.35 ± 0.29
MQ_{LCMC}	41.8	3.04	3.81 ± 0.18	4.93 ± 0.33
MQ_{CMC}	38.1	2.94	3.80 ± 0.08	4.69 ± 0.07
MQ_{CMC}	35.8	2.79	4.40 ± 0.72	5.43 ± 0.96

strong antibacterial activity of the CTAB and its sufficiently high concentration at the surface. Complexity of synthesis method used in previous studies for preparing the antibacterial agents renders these agents non-competitive candidates for manufacturing antibacterial membranes [15–18,28–31,35,36]. In contrast, commercially available CTAB can be used without any need for modification leading to reduction in the cost of fabrication and the difficulty of scale up.

3.4. The stability of the CTAB-containing membrane

The membrane prepared at the CMC showed the meaningful flux and antibacterial activity at the same time, consequently was chosen as the optimum membrane. Leaching experiment was conducted to evaluate the stability of this membrane. For this purpose, first the incorporated CTAB concentration was determined using TGA analysis. As seen in Fig. 10, single stage decomposition was observed for the CTAB below 400 °C [13] and the pristine membrane (M0) between 480 °C and 560 °C. On the other hand, the MQ_{CMC} membrane decomposed in two stages due to the loss of CTAB below 400 °C and the loss of the polymers, PSF and SPES, between 480 °C and 560 °C. Using the weight loss data for the CTAB and the MQ_{CMC}, the loading of CTAB to the membrane was determined as 3.1%. Fig. 11 shows that the release of CTAB continued up to 7 days. At the end of 30 days of storage, a small amount of the CTAB around 4.2% leached from the membrane. This amount corresponds to the free CTAB which did not involve in electrostatic interaction. Zhang et al. [13] reported 30% and 2% losses for the CTAB

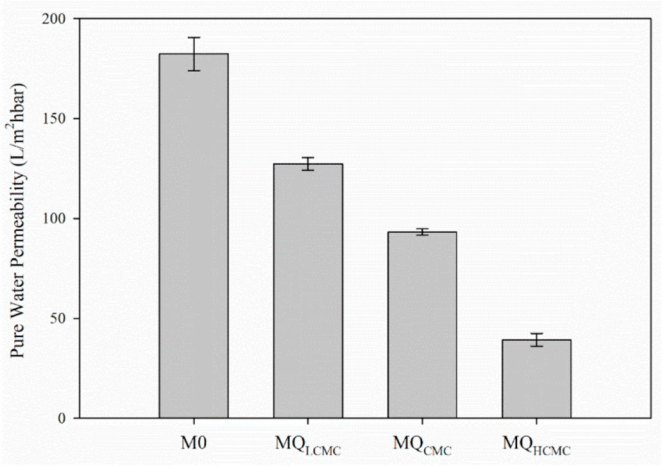

Fig. 7. PWP of the pristine and CTAB modified membranes.

and CTAB@Carbon composites, respectively from polyvinylidene fluoride (PVDF) membrane. They increased the stability of the CTAB by immobilizing it on a carbon support using harsh chemicals and conditions. In our work, the CTAB-containing membrane was prepared in a single step but it was made long-term stable through strong electrostatic interaction between positively charged quaternary ammonium group in CTAB and negatively charged sulfonic acid group in PSF-SPES (Scheme 1).

The strength of the electrostatic binding of the CTAB to SPES was evaluated by storing the membranes in 1 M NaCl solution up to 1 month and by filtering the 1 M NaCl through the membrane. As shown in Fig. 12, the MQ_{CMC} membranes at the end of static storage in NaCl solution or dynamic filtration of NaCl solution showed the same antibacterial activity as compared to their fresh counterparts. The results proved strong electrostatic interaction between the CTAB and SPES since at high salt concentrations in solution, the screening effect of salt

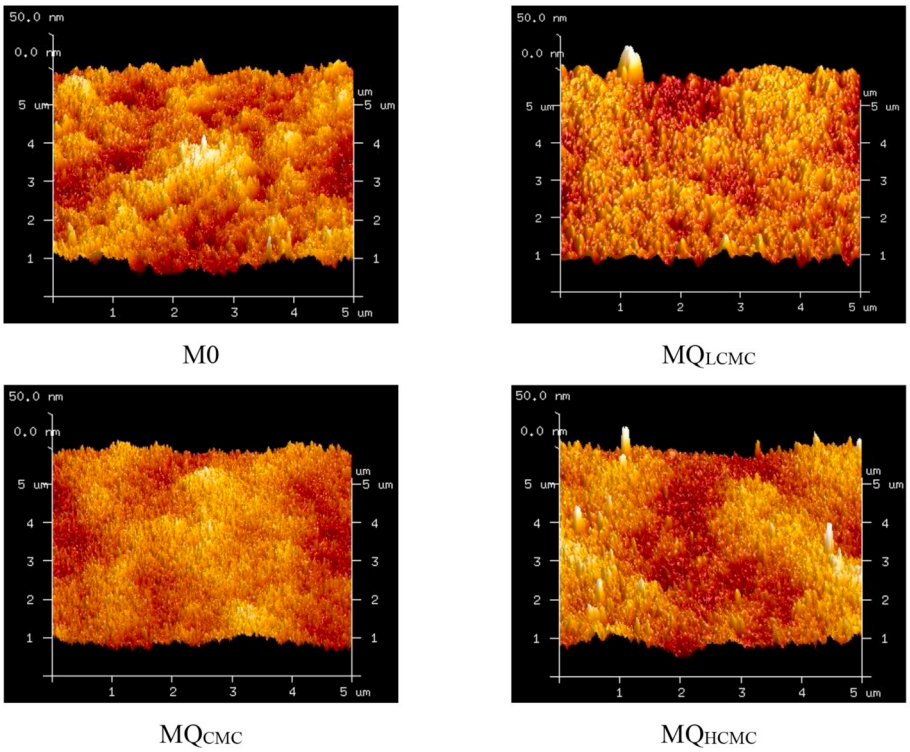

Fig. 6. AFM images of the pristine and CTAB modified membranes.

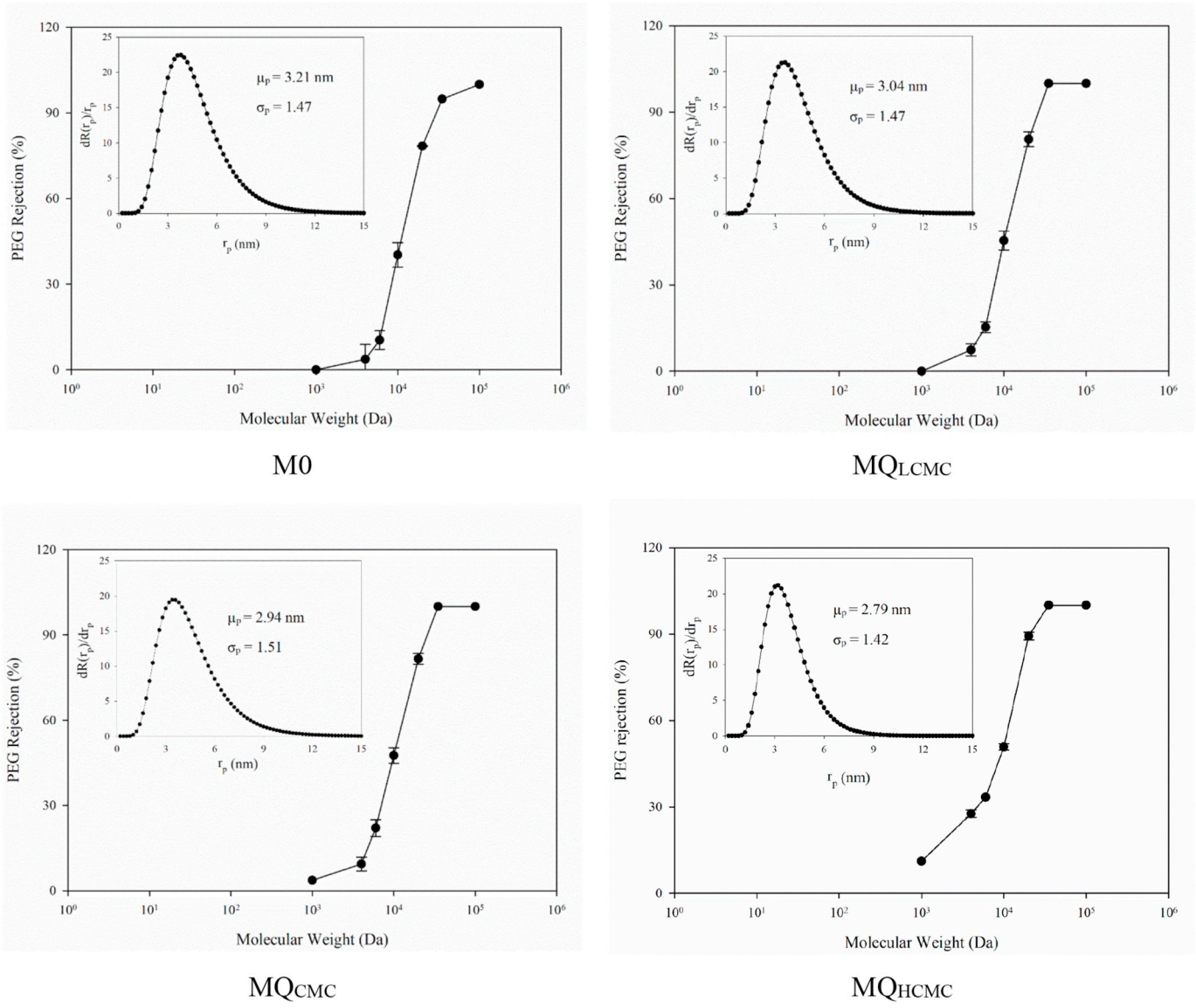

Fig. 8. MWCO of the pristine and CTAB modified membranes.

ions can easily destroy weak electrostatic bond.

3.5. Antibiofouling assessment

The antibiofouling properties of the pristine (M0) and MQ_{CMC} membranes were evaluated using dead-end cell filtration system with two model bacteria suspensions. The initial water flux of the membranes was adjusted to the similar value by controlling transmembrane pressure difference (TMP). As shown in Figs. 13 and 14, the initial flux of the pristine membrane decreased sharply since the bacteria instantaneously deposited on the membrane surface. Following the initial stage, the flux continued to decrease linearly indicating the growth of the biofilm thickness over time. However, a sharp flux decline was not recorded for the MQ_{CMC} membrane at the initial stage of the filtration. The results in Table 5 show that the MQ_{CMC} membrane demonstrated almost 100% flux recoveries following 10 min rinsing with PBS solution after filtration. On the other hand, flux recoveries for the pristine membrane were determined to be 58.3% and 67.4% at the end of *E. coli* and *S. aureus* filtrations. The results indicate that fouling on the surface of the MQ_{CMC} was due to accumulation of dead bacteria, thus, this fouling was reversible and easily removed with simple rinsing. SEM images in Fig. 15 show that many bacteria attached on the surface of the pristine membrane, by contrast, only a few bacteria were observed on the MQ_{CMC}. Myint et al. [40] showed that the roughness and hydrophobicity are important surface properties in determining initial cell adhesion, aggregation and colony formation. Among four nanofiltration membranes investigated, the greatest cell deposition was observed for a membrane which had the most hydrophobic and roughest surface. Our results suggest that in the presence of a strong antibacterial agent on the surface, biofilm formation is not influenced by the roughness, hydrophobicity or surface charge. Although the MQ_{CMC} is more hydrophobic and less negatively charged than the pristine membrane, much higher flux recovery recorded for this membrane is due to its excellent antibacterial activity. The CTAB, mostly accumulated on the surface as confirmed by the XPS analysis (Table 4), reduced bacterial attachment by inactivating bacteria through contact. Table 6 compares the antibiofouling performance of our membrane with that of other ultrafiltration membranes. Previous studies reported a slightly lower flux decline at the end of *E. coli* filtration. However, in these studies a lower bacteria concentration was filtered in a crossflow filtration unit. For comparison, Hou et al. [41] filtered 4.2×10^4 CFU/cm^2 *E. coli* and at the end of filtration they recovered only half of the initial flux (FRR: 58%) after 3 times of washing with water. On the contrary, in our study, the flux recovery was almost 100% although we filtered 100 times more

Table 3
Static antibacterial activity of the ultrafiltration membranes in the literature.

Membranes	Antibacterial agent/ Polymer (wt/ wt, %)	Bacteria concentration (CFU/mL)		Antibacterial rate (%)		Refs.
		E. coli	*S. aureus*	*E. coli*	*S. aureus*	
SiO_2@N-Halamine/ PES	7.5	10^6	–	60.22	–	[28]
HPEI-GO/PES	16.7	10^6	–	74.88	–	[29]
PES/TPQP-Cl	25.0	–	–	76.00	–	[30]
Chitosan/BPPO	–	–	–	70.00	–	[31]
PDA-b-PBA	–	10^6	10^6	92.70	81.30	[32]
PSF/P(H-M-A)	16.7	–	–	89.20	–	[33]
PVDF/N–Si-MWNTs	1.875	10^4	10^5	95.60	98.00	[34]
QPVC	–	–	–	74.20	–	[35]
GO-p-PES	–	10^5	–	80.00	–	[36]
PVDF/MWNTs-g-CDDAC	4.17	10^6	10^6	92.70	95.20	[37]
HNTs-CS@Ag/ PES	3.0	10^6	10^6	94.00	92.60	[38]
MQ_{LCMC}	–	10^6	10^6	87.35	27.50	This work
MQ_{CMC}	3.1			95.78	100	
MQ_{HCMC}	–			99.84	100	

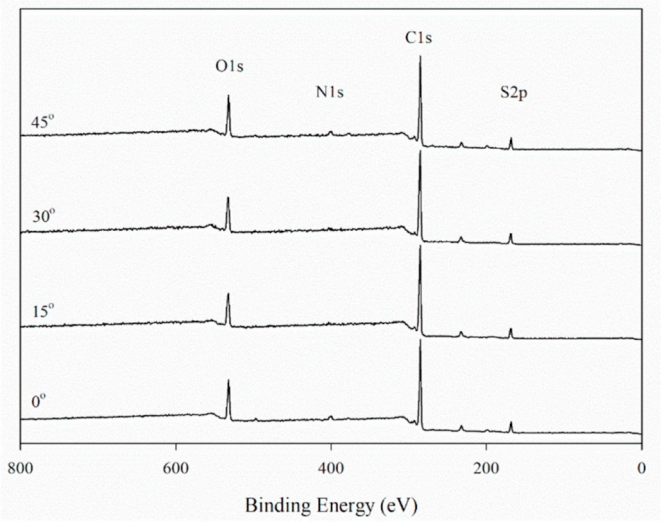

Fig. 9. General XPS survey of the MQ_{CMC} membrane.

Table 4
Surface elemental composition (wt %) of the MQ_{CMC} membrane.

Angle (°)	Surface elemental composition (wt %)				
	C1s	O1s	S2p	N1s	N/C
0	74.62	16.52	5.28	3.58	0.048
15	74.83	16.37	5.02	3.78	0.051
30	74.44	16.52	5.13	3.91	0.053
45	74.60	16.22	5.21	3.97	0.053

concentrated *E. coli* in a dead-end filtration unit. Compared to a cross flow filtration mode, fouling/biofouling occurs at a higher rate in a dead-end filtration unit.

4. Conclusion

In this study, a facile approach is proposed for the fabrication of PSF-SPES blend antibacterial ultrafiltration membranes. The method is based on adding a positively charged quaternary ammonium compound, CTAB, in the gelation medium which makes electrostatic interaction with the SPES mostly at the polymer/bath interface. The presence of CTAB in the membranes was verified by ATR-FTIR and XPS measurements. Compared to the pristine membrane, the CTAB-containing membranes displayed lower hydrophilicity, pure water permeability, MWCO and less negative charge. The membrane prepared at the CMC showed the meaningful flux and antibacterial activity simultaneously, consequently was chosen as the optimum membrane. This membrane had much higher FRR than the pristine membrane following bacteria filtration and rinsing with PBS solution. In addition, the stability of the CTAB in this membrane was proved with leaching experiments and antibacterial activity measurements conducted after storing the membrane in 1 M NaCl up to 1 month and filtering 1 M NaCl

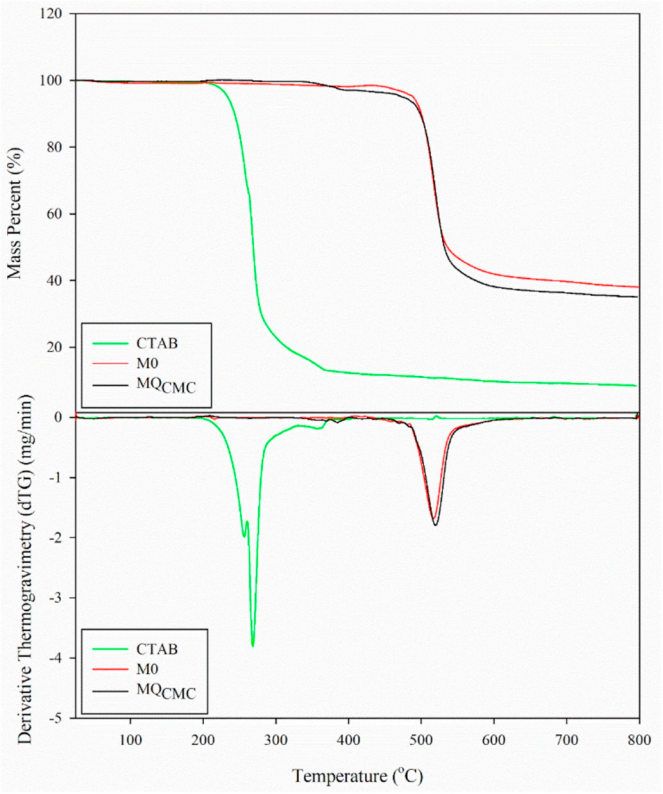

Fig. 10. TGA and dTG analysis of pure CTAB, M0 and MQ_{CMC} membranes as a function of temperature.

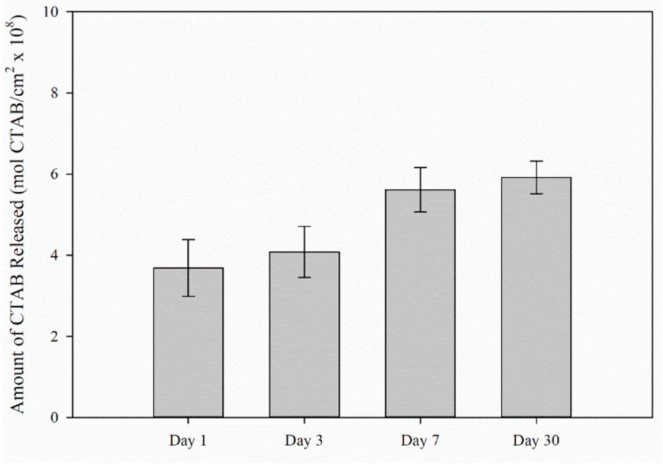

Fig. 11. CTAB release from the MQ_{CMC} membrane as a function of time.

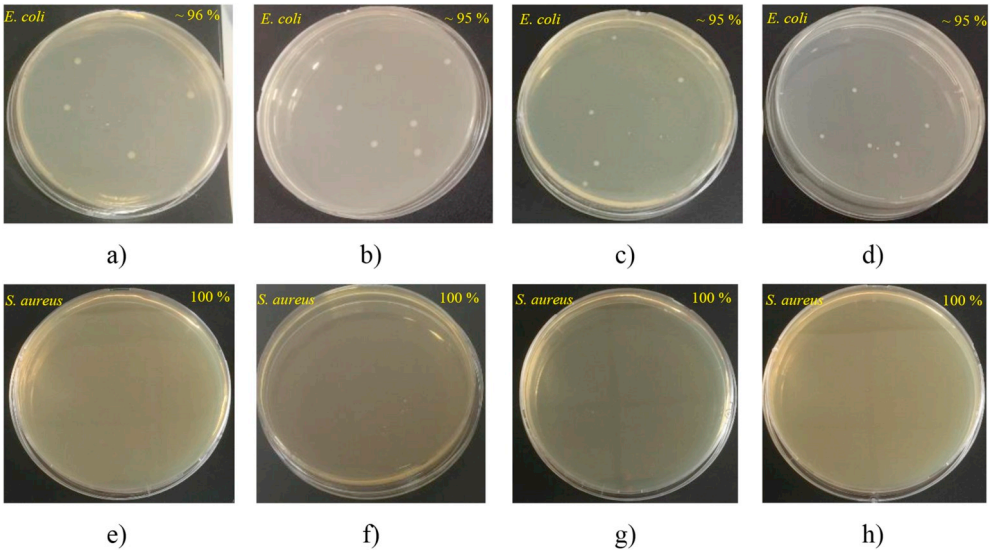

Fig. 12. Bactericidal rates of the (a,e) fresh MQ_{CMC} membrane (b,f) the MQ_{CMC} membrane exposed to 1 M NaCl for two weeks (c,g) the MQ_{CMC} membrane exposed to 1 M NaCl for 1 month (d,h) the MQ_{CMC} membrane after filtration of 1 L of 1 M NaCl solution.

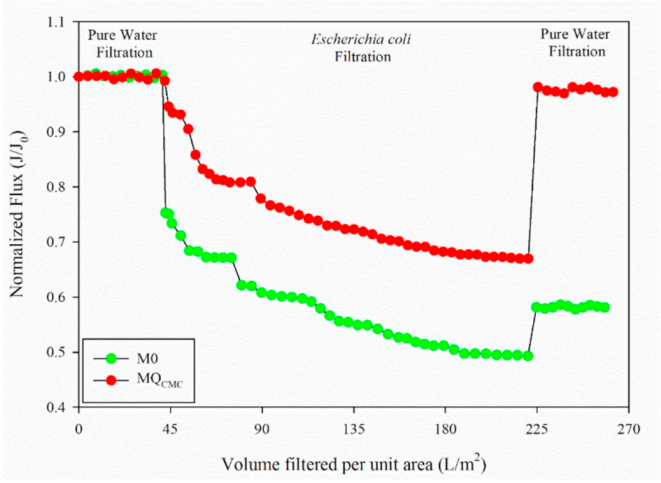

Fig. 13. Normalized flux of the M0 and MQ_{CMC} membranes as a function of volume filtered per unit area during *E. coli* filtration. Initial water fluxes of M0 and MQ_{CMC} membranes are 185 ± 3.5 and 95 ± 2.3, respectively. Transmembrane pressures (TMP) applied for the filtration with M0 and MQ_{CMC} membranes are 0.5 and 1.0 bar, respectively.

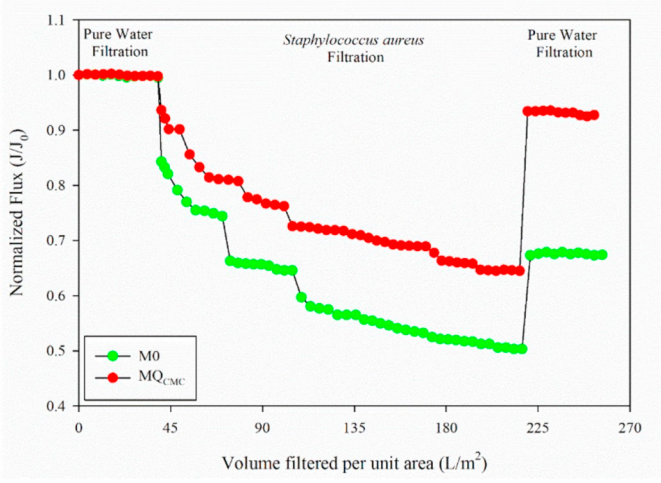

Fig. 14. Normalized flux of the M0 and MQ_{CMC} membranes as a function of volume filtered per unit area during *S. aureus* filtration. Initial water fluxes of M0 and MQ_{CMC} membranes are 185 ± 3.5 and 95 ± 2.3, respectively. Transmembrane pressures (TMP) applied for the filtration with M0 and MQ_{CMC} membranes are 0.5 and 1.0 bar, respectively.

solution.

The key advantages of the membrane developed in this study are the single step preparation using commercially available polymers and antibacterial agent without any need for pre-treatment or post treatment of either the membrane or antibacterial agent and its high antibacterial activity. The facile route proposed in this study can be applied using other polymers and antibacterial agents. The prerequisite for the polymer and antibacterial agent is that they should have functional groups such as hydroxyl, carboxyl, amine and sulfonic groups. In addition to CTAB, electrolytes, other surfactants and antibacterial components can also be used in the coagulation bath as long as they are soluble in water. Although the main driving force used in our study to form a stable long-term interaction between the polymer and the antibacterial agent was electrostatic, other type of strong interactions such as covalent bond can also be utilized. It should also be noted that compositions of both casting solution and coagulation bath should be adjusted in such a way that diffusion rates of the polymer and active agent should be comparable so that most of the interaction between them occurs at the interface.

Overall, the successful preparation of an antibacterial membrane through coagulation in CTAB-containing bath opens opportunities for further investigation in water and wastewater treatment. The stability, high antibiofouling properties and ease of manufacturing make our membrane a potential candidate for these applications. Unlike coating and grafting methods, the facile route proposed in this study can be easily scaled-up to fabricate antibacterial ultrafiltration membranes from commercially available polymers and antibacterial agents without requiring pre or post-treatment steps.

Table 5
Flux recovery ratio and biofouling resistances of the membranes.

Membranes	*E. coli*				*S. aureus*			
	R_{rev} (%)	R_{irrev} (%)	R_{total} (%)	FRR (%)	R_{rev} (%)	R_{irrev} (%)	R_{total} (%)	FRR (%)
M0	4.1	41.7	42.2	58.3	7.2	32.6	39.8	67.4
MQ_{CMC}	22.7	2.4	25.1	97.6	18.8	7.3	25.9	92.7

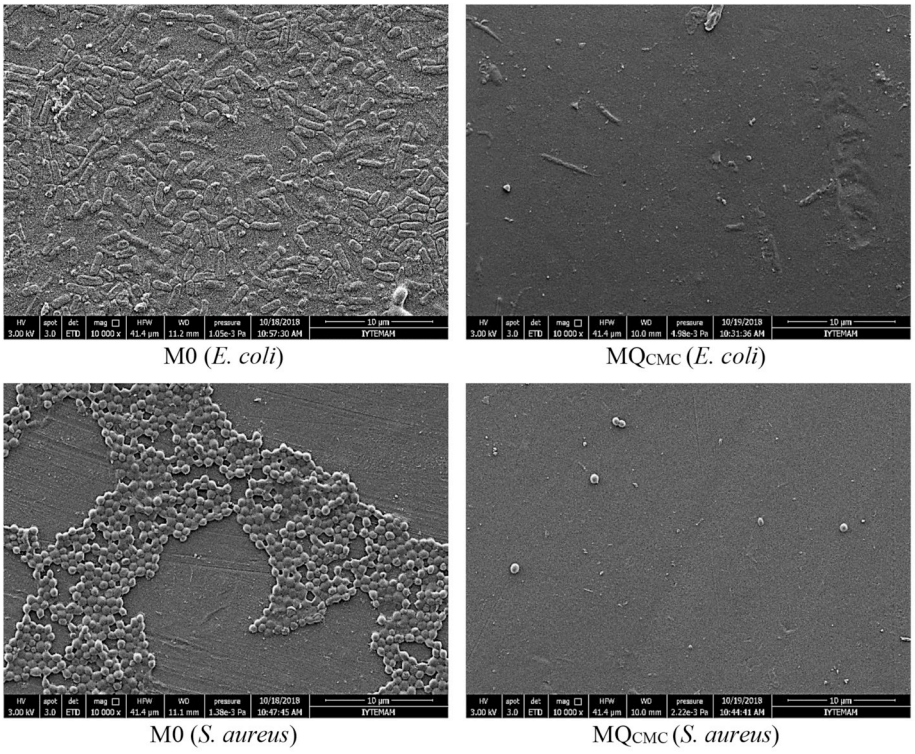

Fig. 15. SEM images of the M0 and MQ_{CMC} membranes after bacteria filtration.

Table 6
Antibiofouling performance of the membranes in the literature.

Membranes	Flow mode	Bacteria concentration (CFU/cm^2)		Flux decline after bacteria filtration (%)		Washing procedure	Flux recovery ratio, FRR (%)		Refs.
		E. coli	*S. aureus*	*E. coli*	*S. aureus*		*E. coli*	*S. aureus*	
GO-p-PES	Cross flow	4.8×10^5	–	~ 25.0	–	–	–	–	[36]
GOQDs-PVDF	Cross flow	~ 1.9×10^5	–	24.3	–	–	–	–	[42]
HPEI-GO/PES	Cross flow	~ 4.5×10^4	–	~ 23.0	–	–	–	–	[29]
PEK-N-Cl	Cross flow	~ 4.2×10^4	–	–	–	Pure water (three times)	58.0	–	[41]
MQ	Dead-end	–	~ 2.6×10^5	–	~ 50.0	–	–	–	[43]
MQ_{CMC}	Dead-end	~ 9.3×10^6	~ 1.2×10^7	~ 33.0	~ 36.0	Deionised water (rinsing 10 min)	97.6	92.3	This work

Acknowledgements

One of the authors, Aydın Cihanoğlu, was supported by the Scientific and Technological Research Council of Turkey (TÜBİTAK) with (2211/E) National PhD Scholarship programme. We also would like to thank the Material Research Center, Biotechnology and Bioengineering Application Research Center and Environmental Research Center at the İzmir Institute of Technology for their kind help and technical support.

References

[1] J. Mansouri, S. Harrisson, V. Chen, Strategies for controlling biofouling in membrane filtration systems: challenges and opportunities, J. Mater. Chem. 20 (2010) 4567–4586.
[2] M.T. Khan, P.Y. Hong, N. Nada, J.P. Croue, Does chlorination of seawater reverse osmosis membranes control biofouling? Water Res. 78 (2015) 84–97.
[3] A. Matin, Z. Khan, S.M.J. Zaidi, M.C. Boyce, Biofouling in reverse osmosis membranes for seawater desalination: phenomena and prevention, Desalination 281 (2011) 1–16.
[4] N. Prihasto, Q.F. Liu, S.H. Kim, Pre-treatment strategies for seawater desalination by reverse osmosis system, Desalination 249 (2009) 308–316.
[5] E.R. Cornelissen, J.S. Vrouwenvelder, S.G.J. Heijman, X.D. Viallefont, D.V.D. Kooij, L.P. Wessels, Periodic air/water cleaning for control of biofouling in spiral wound membrane elements, J. Membr. Sci. 287 (2007) 94–101.
[6] J. Zhu, J. Hou, Y. Zhang, M. Tian, T. He, J. Liu, V. Chen, Polymeric antimicrobial membranes enabled by nanomaterials for water treatment, J. Membr. Sci. 550 (2018) 173–197.
[7] F. Perreault, M.E. Tousley, M. Elimelech, Thin-film composite polyamide

membranes functionalized with biocidal graphene oxide nanosheets, Environ. Sci. Technol. Lett. 1 (2014) 71–76.
[8] S. Kang, M. Pinault, L.D. Pfefferle, M. Elimelech, Single-walled carbon nanotubes exhibit strong antimicrobial activity, Langmuir 23 (2007) 8670–8673.
[9] S. Kang, M. Herzberg, D.F. Rodrigues, M. Elimelech, Antibacterial effects of carbon nanotubes: size does matter, Langmuir 24 (2008) 6409–6413.
[10] A. Munoz-Bonilla, M. Fernandez-Garcia, Polymeric materials with antimicrobial activity, Prog. Polym. Sci. 37 (2012) 281–339.
[11] R. Kaur, S. Liu, Antibacterial surface design-contact kill, Prog. Surf. Sci. 91 (2016) 136–153.
[12] X. Zhang, Z. Wang, M. Chen, M. Liu, Z. Wu, Polyvinylidene fluoride membrane blended with quaternary ammonium compound for enhancing anti-biofouling properties: effects of dosage, J. Membr. Sci. 520 (2016) 66–75.
[13] X. Zhang, Z. Wang, M. Chen, J. Ma, S. Chen, Z. Wu, Membrane biofouling control using polyvinylidene fluoride membrane blended with quaternary ammonium compound assembled on carbon material, J. Membr. Sci. 539 (2017) 229–237.
[14] C. Wu, Z. Wang, S. Liu, Z. Xie, H. Chen, X. Lu, Simultaneous permeability, selectivity and antibacterial property improvement of PVC ultrafiltration membranes via in-situ quaternization, J. Membr. Sci. 548 (2018) 50–58.
[15] J.W. Xu, Y. Wang, Y.F. Yang, X.Y. Ye, K. Yao, J. Ji, Z.K. Xu, Effects of quaternization on the morphological stability and antibacterial activity of electrospun poly (DMAEMA-co-AMA) nanofibers, Colloids Surf., B 133 (2015) 148–155.
[16] P. Fei, L. Liao, J. Meng, B. Cheng, X. Hu, J. Song, Non-leaching antibacterial cellulose triacetate reverse osmosis membrane via covalent immobilization of quaternary ammonium cations, Carbohydr. Polym. 181 (2018) 1102–1111.
[17] X. Zhang, Z. Wang, C.Y. Tang, J. Ma, M. Liu, M. Ping, M. Chen, Z. Wu, Modification of microfiltration membranes by alkoxysilane polycondensation induced quaternary ammonium compounds grafting for biofouling mitigation, J. Membr. Sci. 549 (2018) 165–172.
[18] X. Hu, X. Lin, H. Zhao, Z. Chen, J. Yang, F. Li, C. Liu, F. Tian, Surface functionalization of polyethersulfone membrane with quaternary ammonium salts for contact-active antibacterial and anti-biofouling properties, Materials 9 (2016) 376.
[19] Y. Kakihana, L. Cheng, L.F. Fang, S.Y. Wang, S. Jeon, D. Saeki, S. Rajabzadeh, H. Matsuyama, Preparation of positively charged PVDF membranes with improved antibacterial activity by blending modification: effect of change in membrane surface material properties, Colloids Surf., A 533 (2017) 133–139.
[20] Y. Ma, J. Dai, L. Wu, G. Fang, Z. Guo, Enhanced anti-ultraviolet, anti-fouling and anti-bacterial polyelectrolyte membrane of polystyrene grafted with trimethyl quaternary ammonium salt modified lignin, Polymer 114 (2017) 113–121.
[21] J. Lin, W. Ye, M.C. Baltaru, Y.P. Tang, N.J. Bernstein, P. Gao, S. Balta, M. Vlad, A. Volodin, A. Sotto, P. Luis, A.L. Zydney, B.V. Bruggen, Tight ultrafiltration membranes for enhanced separation of dyes and Na_2SO_4 during textile wastewater treatment, J. Membr. Sci. 514 (2016) 217–228.
[22] Y. Yang, H. Zhang, P. Wang, Q. Zheng, J. Li, The influence of nano-sized TiO_2 filler on the morphologies and properties of PSF UF membrane, J. Membr. Sci. 288 (2007) 231–238.
[23] A.N. Olcay, M. Polat, H. Polat, Ancillary effects of surfactants on filtration of low molecular weight contaminants through cellulose nitrate membrane filters, Colloids Surf., A 492 (2016) 199–206.
[24] R. Matz, The structure of cellulose acetate membranes 1. The development of porous structures in anisotropic membranes, Desalination 10 (1) (1972) 1–15.
[25] R.W. Baker, Membrane Technology and Applications, third ed., John Wiley & Sons, Ltd., New York, NY, 2012.
[26] E.M. Hoek, V.V. Tarabara, Encyclopedia of Membrane Science and Technology, John Wiley & Sons Canada, Limited, Hoboken, NJ, 2013.
[27] L. Coppola, R. Gianferri, I. Nicotera, C. Oliviero, G.A. Ranieri, Structural changes in CTAB/H_2O mixtures using a rheological approach, Phys. Chem. 6 (2004) 2364–2372.
[28] H. Yu, X. Zhang, Y. Zhang, J. Liu, H. Zhang, Development of a hydrophilic PES ultrafiltration membrane containing SiO_2@N-Halamine nanoparticles with both organic antifouling and antibacterial properties, Desalination 326 (2013) 69–76.
[29] L. Yu, Y. Zhang, B. Zhang, J. Liu, H. Zhang, C. Song, Preparation and characterization of HPEI-GO/PES ultrafiltration membrane with antifouling and antibacterial properties, J. Membr. Sci. 447 (2013) 452–462.
[30] K. Wang, X. Lin, G. Jiang, J.Z. Liu, L. Jiang, C.M. Doherty, A.J. Hill, T. Xu, H. Wang, Slow hydrophobic hydration induced polymer ultrafiltration membranes with high water flux, J. Membr. Sci. 471 (2014) 27–34.
[31] Y. Feng, X. Lin, H. Li, L. He, T. Sridhar, A.K. Suresh, J. Bellare, H. Wang, Synthesis and characterization of Chitosan-grafted BPPO ultrafiltration composite membranes with enhanced antifouling and antibacterial properties, Ind. Eng. Chem. Res. 53 (2014) 14974–14981.
[32] X. Wang, S. Jing, Y. Liu, S. Liu, Y. Tan, Diblock copolymer containing bioinspired borneol and dopamine moieties: synthesis and antibacterial coating applications, Polymer 116 (2017) 314–323.
[33] J. Xu, X. Feng, J. Hou, X. Wang, B. Shan, L. Yu, C. Gao, Preparation and characterization of a novel polysulfone UF membrane using a copolymer with capsaicin-mimic moieties for improved anti-fouling properties, J. Membr. Sci. 446 (2013) 171–180.
[34] Y.W. Huang, Z.M. Wang, X. Yan, J. Chen, Y.J. Guo, W.Z. Lang, Versatile polyvinylidene fluoride hybrid ultrafiltration membranes with superior antifouling, antibacterial and self-cleaning properties for water treatment, J. Colloid Interface Sci. 505 (2017) 38–48.
[35] C. Wu, Z. Wang, S. Liu, Z.H. Xie, X. Lu, Simultaneous permeability, selectivity and antibacterial property improvement of PVC ultrafiltration membranes via in-situ quaternization, J. Membr. Sci. 548 (2018) 50–58.
[36] W. Zhang, W. Cheng, E. Ziemann, A. Bear, X. Lu, M. Elimelech, R. Bernstein, Functionalization of ultrafiltration membrane with polyampholyte hydrogel and graphene oxide to achieve dual antifouling and antibacterial properties, J. Membr. Sci. 565 (2018) 293–302.
[37] B. Kang, Y.D. Li, J. Liang, X. Yan, J. Chen, W.Z. Lang, Novel PVDF hollow fiber ultrafiltration membranes with antibacterial and antifouling properties by embedding N-Halamine functionalized multiwalled carbon nanotubes (MWNTs), RSC Adv. 6 (2016) 1710–1721.
[38] Y. Chen, Y. Zhang, H. Zhang, J. Liu, C. Song, Biofouling control of halloysite nanotubes-decorated polyethersulfone ultrafiltration membrane modified with chitosan-silver nanoparticles, Chem. Eng. J. 228 (2013) 12–20.
[39] J.F. Hester, P. Banerjee, A.M. Mayes, Preparation of protein-resistant surfaces on poly(vinylidene fluoride) membranes via surface segregation, Macromolecules 32 (1999) 1643–1650.
[40] A.A. Myint, W. Lee, S. Mun, C.H. Ahn, S. Lee, J. Yoon, Influence of membrane surface properties on the behavior of initial bacterial adhesion and biofilm development onto nanofiltration membranes, Biofouling 26 (2010) 313–321.
[41] S. Hou, X. Dong, J. Zhu, J. Zheng, W. Bi, S. Li, S. Zhang, Preparation and characterization of an antibacterial ultrafiltration membrane with N-Chloramine functional groups, J. Colloid Interface Sci. 496 (2017) 391–400.
[42] Z. Zeng, D. Yu, Z. He, J. Liu, F.X. Xiao, Y. Zhang, R. Wang, D. Bhattacharyya, T.T.Y. Tan, Graphene oxide quantum dots covalently functionalized PVDF membrane with significantly enhanced bactericidal and antibiofouling performances, Sci. Rep. 6 (2016) 20142.
[43] M. Ping, X. Zhang, M. Liu, Z. Wu, Z. Wang, Surface modification of polyvinylidene fluoride membrane by atom-transfer radical-polymerization of quaternary ammonium compound for mitigating biofouling, J. Membr. Sci. 570–571 (2019) 286–293.